https://doi.org/10.1007/s41230-018-8064-8

Tensile behavior of Ti-6Al-4V alloy fabricated by selective laser melting: effects of microstructures and as-built surface quality

Pan Tao[1,2,3], Huai-xue Li [2,3], Bai-ying Huang [2,3], Quan-dong Hu [2,3], Shui-li Gong[2,3], and *Qing-yan Xu [1]

1. Key Laboratory for Advanced Materials Processing Technology (MOE), School of Materials Science and Engineering, Tsinghua University, Beijing 100084, China;

2. Science and Technology on Power Beam Processes Laboratory, AVIC Manufacturing Technology Institute, Beijing 100024, China;

3. Key Laboratory of Aeronautical Technology on additive manufacturing, AVIC Manufacturing Technology Institute, Beijing 100024, China

Abstract: Selective laser melting (SLM) is a powerful additive manufacturing (AM) technology, of which the most prominent advantage is the ability to produce components with a complex geometry. The service performances of the SLM-processed components depend on the microstructure and surface quality. In this work, the microstructures, mechanical properties, and fracture behaviors of SLM-processed Ti-6Al-4V alloy under machined and as-built surfaces after annealing treatments and hot isostatic pressing (HIP) were investigated. The microstructures were analyzed by optical microscope (OM), scanning electron microscope (SEM) and transmission electron microscopy (TEM). The mechanical properties were measured by tensile testing at room temperature. The results indicate that the as-deposited microstructures are characterized by columnar grains and fine brittle martensite and the as-deposited properties present high strength, low ductility and obvious anisotropy. After annealing at 800–900°C for 2–4 h and HIP at 920°C/100MPa for 2 h, the brittle martensite could be transformed into ductile lamellar (α+β) microstructure and the static tensile properties of SLM-processed Ti-6Al-4V alloys in the machined condition could be comparable to that of wrought materials. Even after HIP treatment, the as-built surfaces could decrease the ductility and reduction of area of SLM-processed Ti-6Al-4V alloys to 9.2% and 20%, respectively. The crack initiation could occur at the columnar grain boundaries or at the as-built surfaces. The lamellar (α+β) microstructures and columnar grains could hinder or distort the crack propagation path during tensile tests.

Key words: selective laser melting; Ti-6Al-4V; microstructure; mechanical properties; fracture; surface quality

CLC numbers: TG146.23/136 **Document code:** A **Article ID:** 1672-6421(2018)04-243-10

Ti-6Al-4V is a typical α+β duplex-phase titanium alloy with outstanding specific strength, corrosion resistance and bio-compatibility, which has been widely applied in biomedical, aerospace, automotive, energy, chemical, and other industries [1]. However, the poor machinability and high cost of Ti-6Al-4V using a traditional processing route limit its more extensive application. Furthermore, the production of titanium alloy by conventional processing technology leads to high material waste and greater energy consumption. Therefore, researchers pay more and more attention to non-traditional processing technologies of titanium alloy, such as additive manufacturing (AM) technologies.

Selective laser melting (SLM) is one of the popular powder bed fusion AM processes, which melts fine metal powder particles into near fully dense components by a computer-controlled high-energy laser beam. With respect to conventional manufacturing processes, SLM possesses several obvious advantages such as free of molds, high material utilization, high efficiency delivery, low carbon emissions, and near net shaping production. Besides, owing to its layer-wise production, the SLM process enables the fabrication of geometrically highly complex components which cannot be accomplished by traditional processing technology routes. The SLM process currently has been applied in injection molds, medical equipment and aerospace to fabricate various

***Qing-yan Xu**

Male, born in 1971, Ph.D, professor. His current research mainly focuses on a wide range of topics within the fields of mechanical engineering, manufacturing process, materials engineering, and integrated computational materials engineering. He is an author/co-author of over 100 peer-reviewed journals/conference papers, 5 edited books, and 6 patents.

E-mail: scjxqy@tsinghua.edu.cn

Received: 2018-05-09; Accepted: 2018-06-19

complicated components such as molds with cooling channels, patient customized implants and optimized structures for weight reduction. After years of effort, the Ti-6Al-4V alloy with a relative density up to 99.99% could be obtained using optimized SLM process parameters. Nevertheless, due to the special physical metallurgical process derived from high energy density and small beam diameter, the microstructure of SLM-built Ti-6Al-4V alloy is different from that of the counterparts through traditional methods. The columnar prior-β grains parallel to building direction, which have been demonstrated by many previous papers [2-6], contribute to the obvious anisotropy in as-deposited properties. For high cooling rate in SLM, the as-built Ti-6Al-4V alloy microstructure mainly consists of fine non-equilibrium martensite, resulting in higher strength than conventional Ti-6Al-4V material but poor ductility [3]. In addition, a high residual stress usually exists in SLM-processsed parts after deposition [7].

To achieve a desired balance of strength and ductility, researchers have made great efforts to regulate the microstructures and properties of SLM-produced titanium alloy in the past few years. Xu et al. [8] adjusted the SLM process parameters to decompose the martensite using in-situ heat treatments and obtained a fine lamellar α+β microstructure and good performances of SLM-built Ti-6Al-4V alloy. The parameters used in their research had the characteristics of high energy density and double scanning, which increased the laser exposure time and the energy transferred to the solidified layers. Nevertheless, this method decreases the processing efficiency and may not be suitable for industrial production. Ali et al. [9] applied a higher pre-heating temperature during SLM of Ti-6Al-4V alloy and found that the in-built residual stresses could be removed and the ductility could be improved significantly when the baseplate was preheated to 570 °C. High temperature pre-heating could reduce the temperature gradient effectively and allow the cooling process during SLM to be well controlled, but there are no high pre-heating components in most SLM machines. At present, post-deposition heat treatments are still effective measures to tailor the microstructures and properties of SLM-fabricated Ti-6Al-4V alloy. The common heat treatments mainly include stress-relief annealing [10], annealing below β-transus temperature [11], hot isostatic pressing (HIP) [4] and two-stage heat treatment of solution followed by aging [12]. However, previous studies mainly focused on the residual stress, microstructure evolution and corresponding mechanical properties of SLM-processed Ti-6Al-4V alloy after heat treatments and machining. After HIP treatment and machining, the mechanical properties of SLM-processed Ti-6Al-4V alloy shows more competitive than that of wrought material.

In addition to the mechanical properties and microstructures, another major challenge for large-scale industrialization of metal SLM process is low surface quality. In the powder bed fusion AM process, the poor surface finish arises from the stair-stepping effect and bonding of powder particles. Many optimized geometric designs for SLM have complex internal structures such as complex cavities or inner flow channels. To achieve a high surface finish at the outer surface, milling and sand blasting are commonly employed. However, it is difficult to improve the surface quality of every inner surface by machining or milling. So, the service performances of components with inner structures depend on both the microstructure and surface quality. Although it is generally known that a rough surface can deteriorate the mechanical properties of metallic components, there are limited studies [13, 14] on the effects of surface roughness on the mechanical properties of SLM-produced Ti-6Al-4V alloy. In addition, due to the differences in powder and SLM machines, extensive testing is required even if the investigations on the heat treatment of SLM-processsed Ti-6Al-4V alloy have been performed. Therefore, the aim of this paper is to determine the effects of microstructure and as-built surface on tensile properties of SLM-processsed Ti-6Al-4V alloy. Additionally, the tensile fracture mechanism under different microstructure and surface condition was analyzed in depth. Our research results can provide a reference for the part design of SLM-processsed Ti-6Al-4V from the perspective of surface quality.

1 Experimental details

In the current work, a commercial spherical pre-alloyed Ti-6Al-4V powder with a normal size distribution ranging from 23 μm to 56 μm was utilized. The nominal chemical composition (wt. %) of Ti-6Al-4V alloy powder is listed in Table 1. An EOS 280 SLM system was employed to fabricate a number of horizontal and vertical samples as shown in Fig. 1. The SLM machine is equipped with a continuous fiber laser which possesses a maximum laser power of 400 W and a laser spot size of 100 μm. The building process was performed using laser power of 280 W and scanning speed of 1,200 mm·s^{-1} in an argon protective atmosphere lower than 0.1% oxygen content with a constant substrate temperature of 35 °C. The powder layer thickness was set to 30 μm and the hatch distance was 140 μm. To reduce residual stress, the meander scanning pattern was applied and the scanning direction was rotated by 67° after each layer deposition. Under the above process parameters, fully dense Ti-6Al-4V alloy products could be obtained. After building, the as-built samples were separated from the base plate by a wire electrical discharge machining (WEDM). To control the microstructures and mechanical properties, the as-fabricated samples were subjected to various heat treatments. The heat treatments were carried out in a vacuum furnace with a vacuum degree about 1×10^{-3} Pa and a heating rate of about 10 °C·min^{-1}. The detailed heat treatment processes are listed in Table 2. After heat treatments, tensile testing was conducted at room temperature to assess the mechanical properties. At least three specimens were tested for each process condition and building direction. Tensile specimens were machined with a gauge length of 25 mm and a diameter of 5 mm according to GB/T 228-2010 [15]. Tensile tests were performed with a crosshead speed of 1.5 mm·min^{-1} using a universal tensile testing machine equipped with extensometer. Following tensile testing, the fracture surface of the tensile specimens was analyzed by

scanning electron microscopy (SEM) to investigate the fracture mechanism. One half of some fractured tensile specimens was cross-sectioned along the central axis and then prepared as metallographic samples to examine the crack path. To evaluate microstructural features, metallographic specimens were prepared using traditional mechanical grinding, polishing and etching with Kroll reagent. The microstructure characteristics of the as-deposited and heat-treated Ti-6Al-4V alloy specimens were characterized by a Zeiss optical microscope (OM) and SEM. To reveal the microstructural characteristics of as-deposited Ti-6Al-4V alloy in depth, detailed microstructural observations were carried out on an FEI Tecnai-G2 transmission electron microscope (TEM).

Table 1: Chemical composition of Ti-6Al-4V alloy powder used in this experiment (wt. %)

Al	V	Fe	C	N	H	O	Ti
5.5–6.75	3.5–4.5	≤0.30	≤0.10	≤0.05	≤0.015	≤0.20	Bal.

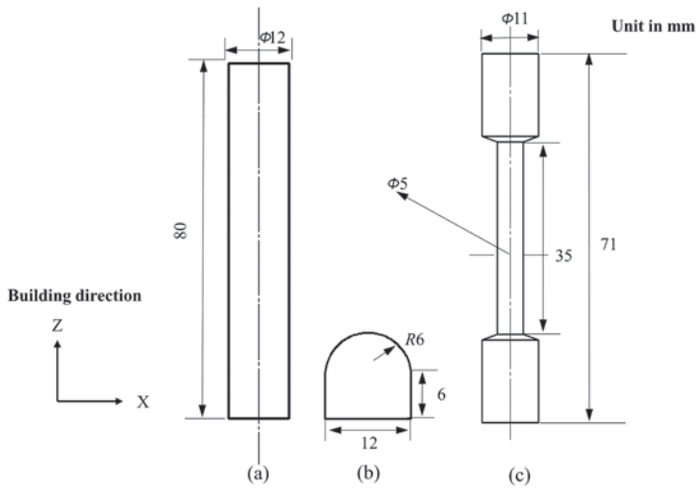

Fig. 1: Schematic of longitudinal section of horizontal (b) and vertical (a/c) samples fabricated by SLM
(Note: The length of the horizontal (b) samples is 80 mm. The samples (a) and (b) were machined into standard tensile testing specimens after heat treatments. The as-built surface in the middle region of the samples (c) was remained. The Z direction was the building direction.)

Table 2: Heat treatment processes for Ti-6Al-4V alloy samples produced by SLM

Samples	Building direction	Heating Temperature (°C)	Soaking time (h)	Cooling method	Surface appearanc
SLM+HT (650°C-2h)	V/ H	650	2	FC	Machined
SLM+HT (800°C-2h)	V/ H	800	2	FC	Machined
SLM+HT (800°C-4h)	V/ H	800	4	FC	Machined
SLM+HT (900°C-2h)	V/ H	900	2	FC	Machined
SLM+HIP (920°C-2h)	V	920	2	FC	As-built
	V/ H	920	2	FC	Machined

For ease of description, the heat-treated samples will be named according to the specific heat treatment process. For "SLM+ HT (800°C-2h)", it means that the specimens were produced by SLM and then heated to 800°C for 2 h. The HIP was carried out at 920°C/100MPa for 2 h. FC is furnace cooling and V/H refers to the vertical/horizontal building directions.

2 Results and discussion

2.1 Microstructural characterization

Microstructural characteristics of the as-deposited Ti-6Al-4V alloy are described in Fig. 2. As the 3D optical metallographic image shown in Fig. 2(a), the parts are nearly free of defects under the current process parameters. The microstructure of as-fabricated Ti-6Al-4V alloy is dominated by columnar prior β grains. The prior β grains grow across several deposited layers and tend to be oriented along with the building direction. The columnar prior β grains arise from the epitaxial growth of the prior β grains in previous layers due to the high temperature gradient and solidification rate in the molten pool. The average width of columnar grains is about 139.7±11.2 μm. Because of an extremely high cooling rate in the range of 10^5–10^6 °C·s^{-1} during SLM [2], the prior β phases are completely transformed to martensitic α′ phases. The columnar prior β grains are filled with very fine martensitic α′ needles as delineated in Fig. 2(b). The TEM observations of the martensitic substructure are shown in Fig. 2(c-d). The α′ martensite lamellae containing high-density dislocations are staggeredly distributed in the matrix. Fine martensite laths are found in the thick α′ martensite lamellae as displayed in Fig. 2(c). Yang et al. [5] investigated the characteristics of martensite in SLM-built Ti-6Al-4V alloy. They found similar phenomenon referred to as martensitic hierarchical structures and believed that the hierarchical structures of martensitic α′ needles depended on the multi-thermal cycles during SLM. As expected, large amounts of twins were observed as displayed in Fig. 2(d). Plastic deformation of close-packed hexagonal crystals such as Ti-6Al-4V alloy is usually accompanied by twinning and dislocation slipping due to fewer slip systems. Due to the severe temperature gradient and high cooling rate, great internal stress will be usually induced in the SLM-fabricated parts. If the internal stress arrives at the critical shear stress of twinning, twinning deformation occurs, resulting in the formation of twins [16].

It is well-established that the mechanical responses of the material are closely related to the microstructure. The

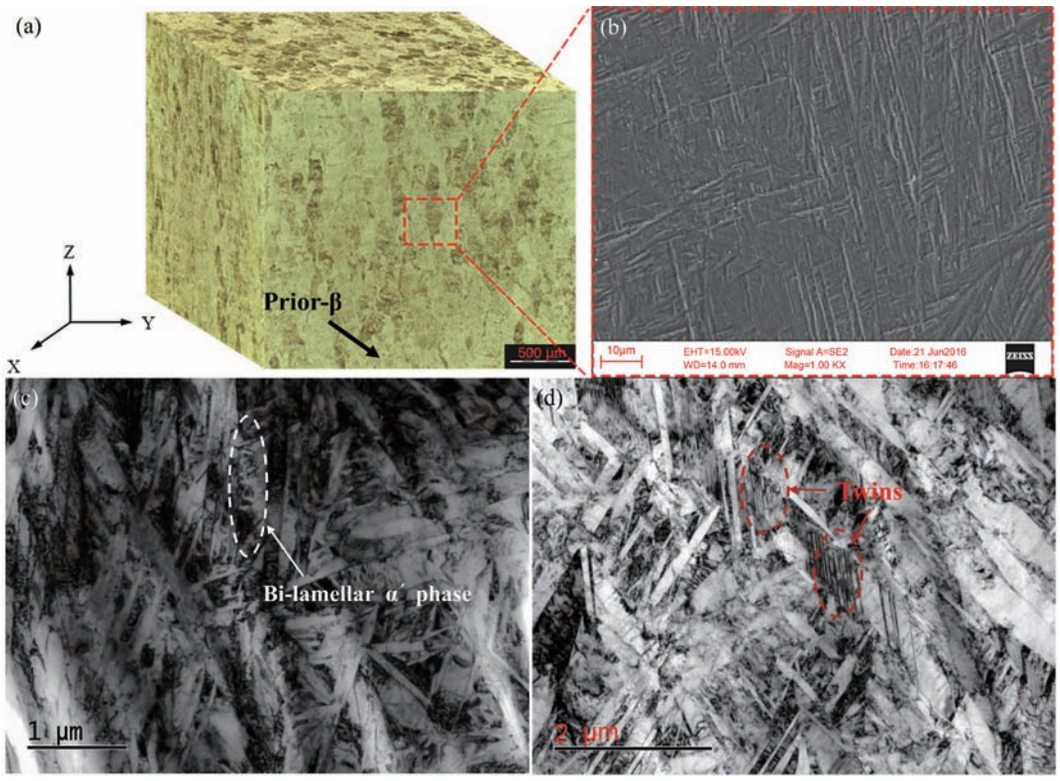

Fig. 2: Microstructure characteristics of as-built Ti-6Al-4V alloy: (a) three-dimensional OM image, (b) SEM image, (c) and (d) TEM images showing detailed microstructure features

martensite α′ phase is a metastable phase, which cannot be acceptable for practical structural applications. Therefore, it is of interest to adopt post-fabrication heat treatment to obtain homogeneous and stable microstructure. Figure 3 shows the microstructures of Ti-6Al-4V alloy samples after various post-SLM heat treatments. When the samples annealed at 650 °C for 2 h, α phases nucleated and grew in the boundaries of some martensitic needles or at dislocations, and a small portion of the martensite phase decomposed into equilibrium α+β phase. The needle-like structure was still remained in the microstructure due to the microstructure hereditary. The decomposition of the martensite resulted in alloy element redistribution.

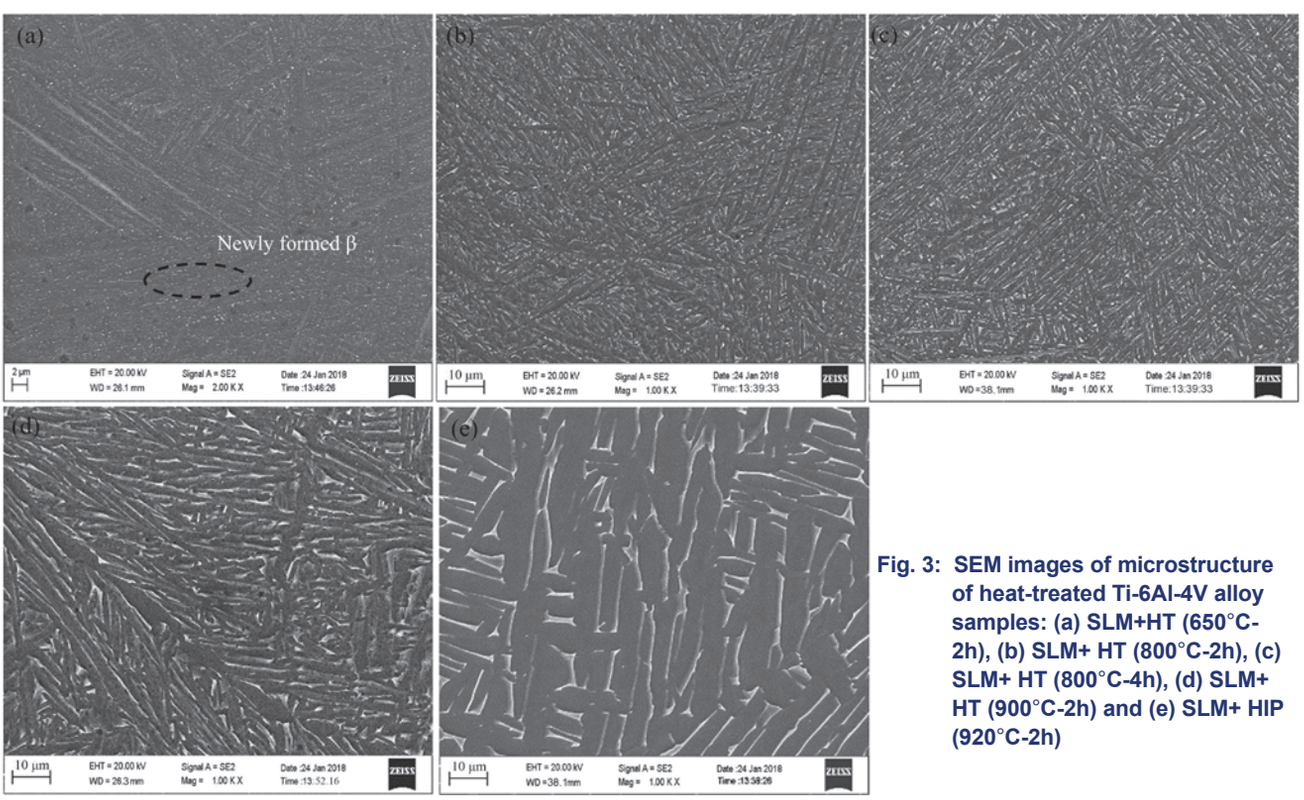

Fig. 3: SEM images of microstructure of heat-treated Ti-6Al-4V alloy samples: (a) SLM+HT (650°C-2h), (b) SLM+ HT (800°C-2h), (c) SLM+ HT (800°C-4h), (d) SLM+ HT (900°C-2h) and (e) SLM+ HIP (920°C-2h)

The V element was enriched in β phases and the Al element was enriched in α phases. The difference of atomic number between alloying elements gives rise to the difference of phase contrast between α and β phases [11]. It can be observed in Fig. 3(a) that the light regions are the newly transformed β phases. While heating to 800 °C for 2 h, the fine martensite α′ phases completely disappeared in the microstructure, and decomposed into equilibrium laminar α and β phases as shown in Fig. 3(b). It was mentioned in previous studies [17] that the upper-limit temperature of martensite decomposition in Ti-6Al-4V is about 800 °C, meaning that the martensite completely decomposes into α and β phases when the heat treatment temperature is above this temperature. Although it is beneficial to the diffusion of alloy elements and coarsening of microstructure for longer holding time during heat treatments, there appears to be no significant changes in the microstructure of the samples after incubation at 800 °C for 4 h as shown in Fig. 3(c). For the low diffusivity of V element in β phases, the coarsening of lamellar in Ti-6Al-4V alloy is mainly controlled by the diffusion of V element. Hence, it is the annealing temperature that plays a more significant role in the coarsening of the laminae relative to annealing time for sub-β-transus heat treatments [18]. As the annealing treatment temperature increased, the width of α phase lath increased. The average width of α phase lath was about 2 μm after annealing at 900 °C as shown in Fig. 3(d). After HIP at 920°C/100MPa, the pores in the Ti-6Al-4V alloy samples were closed, and meanwhile the average width of α phase plates was increased to about 4.1 μm.

2.2 Mechanical properties

Figure 4 shows the tensile testing results for heat-treated and as-deposited Ti-6Al-4V alloy samples with machined surface. It is obvious that the strength of as-deposited Ti-6Al-4V alloy is far beyond the minimum strength requirement of wrought material according to ASTM F1472-14 [19] due to complete martensitic microstructure, very fine grains and high-density crystal defects. However, the elongation of as-built Ti-6Al-4V alloy is relatively poor, with an average value of 6.5%–8.5%, which is lower than the minimum elongation requirement specified in this standard. The brittle martensitic microstructure and the presence of residual stress should be responsible for the lower ductility. After stress relief annealing, the strength and standard deviation of elongation to failure decreased slightly, but the elongation was not significantly improved. When annealing at 650 °C for 2 h, most of the residual stress could be eliminated. However, only partial martensite decomposition was involved,

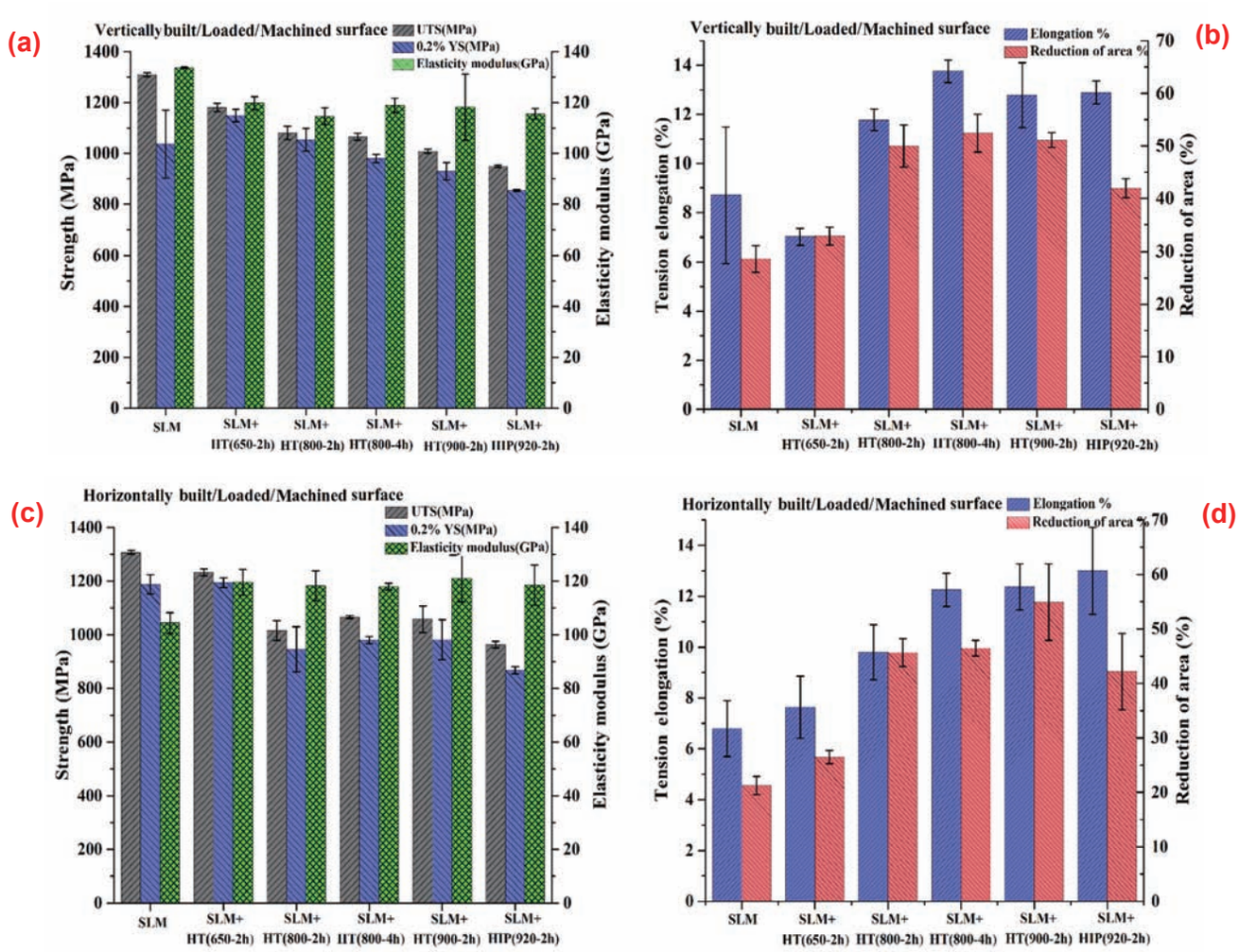

Fig. 4: Tensile properties of heat treated and as-deposited Ti-6Al-4V alloy samples under different tensile orientations: (a) (b) vertically built, (c) (d) horizontally built

and the dominant microstructures were still martensitic phases. Consequently, it plays a limited role in the improvement of mechanical properties. After heat treatment at 800 °C for 2 h, the yield strength (950–1,050 MPa) and ultimate tensile strength (1040–1,080 MPa) show a slight reduction but the ductility is greatly improved to 9.8%–11.8%, as compared with stress relief annealing. The enhanced ductility is attributed to the complete decomposition of martensite into fine lamellar α+β equilibrium phases. In addition, the heat treatment temperature is relatively low so that the coarsening of microstructure is not obvious. For longer residence time at 800 °C, the yield strength presented a slight reduction to 945–980 MPa, but the total elongation increased to 12.3%–13.8%. The enhanced elongation could be ascribed to alloy element redistribution after prolonged annealing. The diffusion of solute leads to increased contents of aluminum in α phases and vanadium in β phases, which induces the microstructure softening [20]. While a higher temperature annealing of 900 °C for 2 h was applied, there was a further reduction of the yield strength to 930–980 MPa. After HIP treatment, the yield strength presented a large decrease to 853–868 MPa. For Ti-6Al-4V alloy with lamellar microstructure, the strength mainly depends on the effective slip length. The strength of titanium alloy increases with the decreasing of the effective slip length. The slip length is equal to the width of α phase lamellae [21]. With the increasing of the annealing temperature below β-transus temperature, the width of α phase plates gradually increases, which leads to a decrease in the strength. In general, the tensile properties of SLM-fabricated Ti-6Al-4V alloy with machined surface after proper post-building heat treatments show comparable to the wrought counterparts.

The mechanical anisotropies are not conducive to the widespread application of SLM-produced components. To assess the anisotropy of mechanical properties, the following equation [22] was used to calculate the differences of tensile properties between horizontally and vertically SLM-built samples:

$$Dr = \frac{|TP_V - TP_H|}{|TP_V + TP_H|/2} \times 100\% \quad (1)$$

where Dr indicates the differences ratio of tensile properties, TP_H and TP_V represent the average tensile mechanical properties of horizontally and vertically built specimens, respectively. The anisotropy of tensile properties of the as-deposited and heat-treated Ti-6Al-4V alloy is summarized in Table 3. It could be clearly observed that there is a strong anisotropy in tensile properties of the as-deposited samples, especially for the ductility. Previous research [23] showed that there was a remarkable lack of ductility in the vertically built specimens because of lack-of-fusion defects. This type of defects has sharp corners and seems to be thin crack perpendicular to the vertical direction. When the tensile load is applied in the vertical direction, the incomplete fusion pores could reduce load-bearing area and result in stress concentration. So the achieved ductility in the vertical direction is poor. However, the ductility in the vertical direction in the present study is higher due to lack of defects. The columnar structures should be responsible for the anisotropy in ductility between the horizontal and vertical directions of the samples. The tension is parallel to the columnar grains in vertically built samples but perpendicular to that in horizontally built samples. The different orientations between columnar grains and loading direction lead to fewer effective grain boundaries to hinder the growth of cracks in the horizontal direction [24]. Thus, a lower elongation is obtained in the horizontally built specimens. As expected, heat treatments could effectively alleviate the anisotropy of mechanical properties. Despite the fact that the variation of anisotropy in each mechanical property is not synchronized with the annealing temperature, the anisotropy decreases with the increasing annealing temperature generally. After HIP treatment, the anisotropy is minimum due to the closure of defects and elimination of residual stresses under the effect of high temperature and pressure. In addition, it is worth pointing out that the anisotropy of ductility is stronger than that of strength, which could be because the ductility of the material is more sensitive to microstructure, defects and residual stress. Meanwhile, the anisotropy of elasticity modulus is mainly affected by the residual stress and not sensitive to the microstructure.

Table 3: Anisotropy of tensile properties of SLM-built Ti-6Al-4V alloy before and after heat treatments

No.	Dr_{UTS}%	Dr_{YS}%	Dr_{EM}%	Dr_{EL}%	Dr_{AR}%
SLM	0.15	13.59	24.69	24.84	29.34
SLM+HT(650°C-2h)	4.29	3.86	1.45	8.36	21.63
SLM+ HT(800°C-2h)	6.21	10.83	3.04	18.29	9.04
SLM+ HT(800°C-4h)	0.03	0.05	0.84	11.58	12.05
SLM+ HT(900°C-2h)	4.84	5.37	2.33	3.29	7.24
SLM+ HIP(920°C-2h)	1.43	1.68	2.56	0.82	0.55

Note: UTS is ultimate tensile strength, YS is yield strength, EL is elongation, EM is elasticity modulus and AR is reduction of area.

In the laser powder bed fusion process, poor surface quality is one of its intrinsic features. The performance of the parts depends on not only the microstructure but also the surface quality, especially for parts with complex cavities or internal flow channels. The tensile mechanical properties of unmachined and machined samples are shown in Fig. 5. It could be seen clearly that the rough surface deteriorates the toughness of SLM-processed samples. The ductility of samples with as-built surfaces cannot meet the standard of the forging, even after HIP processing. For HIP-processed samples with as-built surfaces, the elongation and the reduction of area are about 9.2% and 20%, respectively. With respect to the machined ones, the elongation and the reduction of area are decreased by 28% and 52%, respectively, due to the surface roughness. Figure 6 shows the surface topography of as-built and machined Ti-6Al-4V specimens after tensile tests. For as-built surface, single powder particle or clusters of metallic particles could be observed

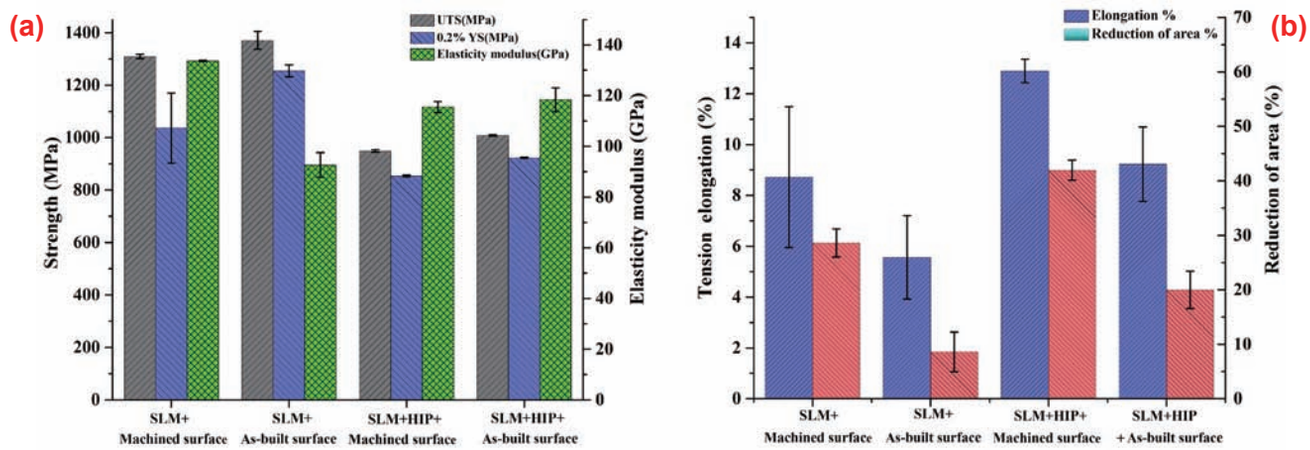

Fig. 5: Tensile properties of heat treated and as-deposited of Ti-6Al-4V alloy with machined and as-built surface: (a) strength and elasticity modulus, (b) ductility

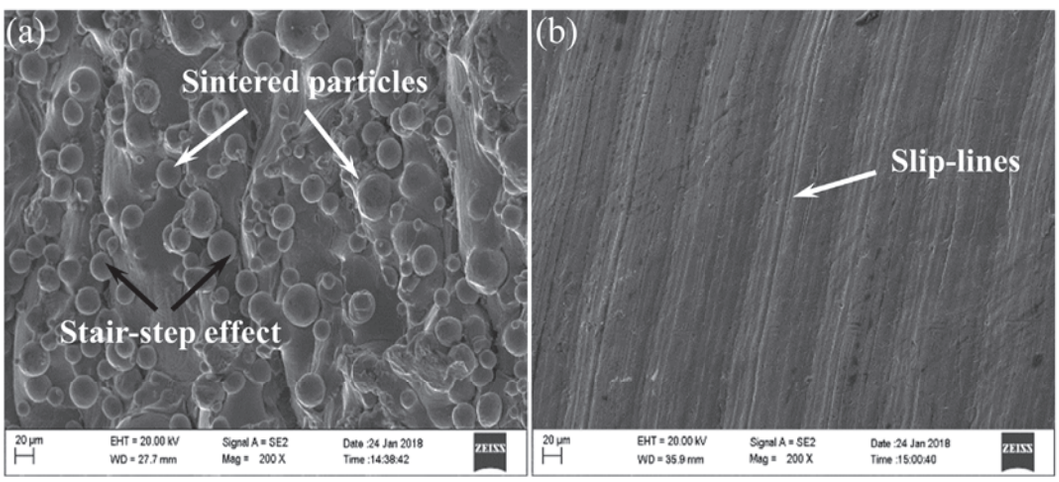

Fig. 6: SEM surface images of as-built and machined Ti-6Al-4V specimens after tensile tests

obviously as shown in Fig. 6(a). These adhesive powder particles arise from the particles at the boundary being partially melted by laser due to insufficient energy. These bonded powder particles could form sharp corner transition regions which act as stress concentrators which lead to decreased ductility. On the other hand, large numbers of slip bands exist on the machined surface as shown in Fig. 6(b), which are the result of polycrystalline plastic deformation. In spite of the decreased ductility, the strength has a small increase relative to machined samples as shown in Fig. 7, which is opposite to previous studies [25]. The increased strength induced by surface roughness may be ascribed to the increased cross-sectional area due to the bonded powder particles.

2.3 Fracture behavior analysis

To gain more insight into the variations of mechanical properties, the tensile fracture surface morphologies of all the specimens were observed by SEM and some representative photographs of the fracture surface of SLM-fabricated Ti-6Al-4V alloy are shown in Fig. 8. Overall, the macroscopic morphologies of tensile fractography in the specimens are dominated by cup-and-cone profiles mainly including shear lip and fiber zone, which indicate typical ductile fractures. The fiber

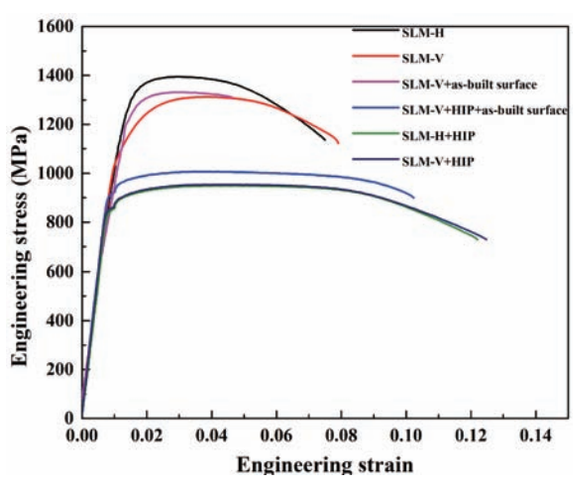

Fig. 7: Engineering stress-strain curves of as-deposited and HIPed Ti-6Al-4V alloy samples showing the effect of microstructure and surface roughness on strength and ductility

zone was circular in the machined specimens as indicated in Fig. 8(a_0-b_0), while the fiber zone in specimens with as-built surface is approximately ellipsoidal and a long axis of the ellipse-like fiber zone is attached to the surface of the sample as displayed

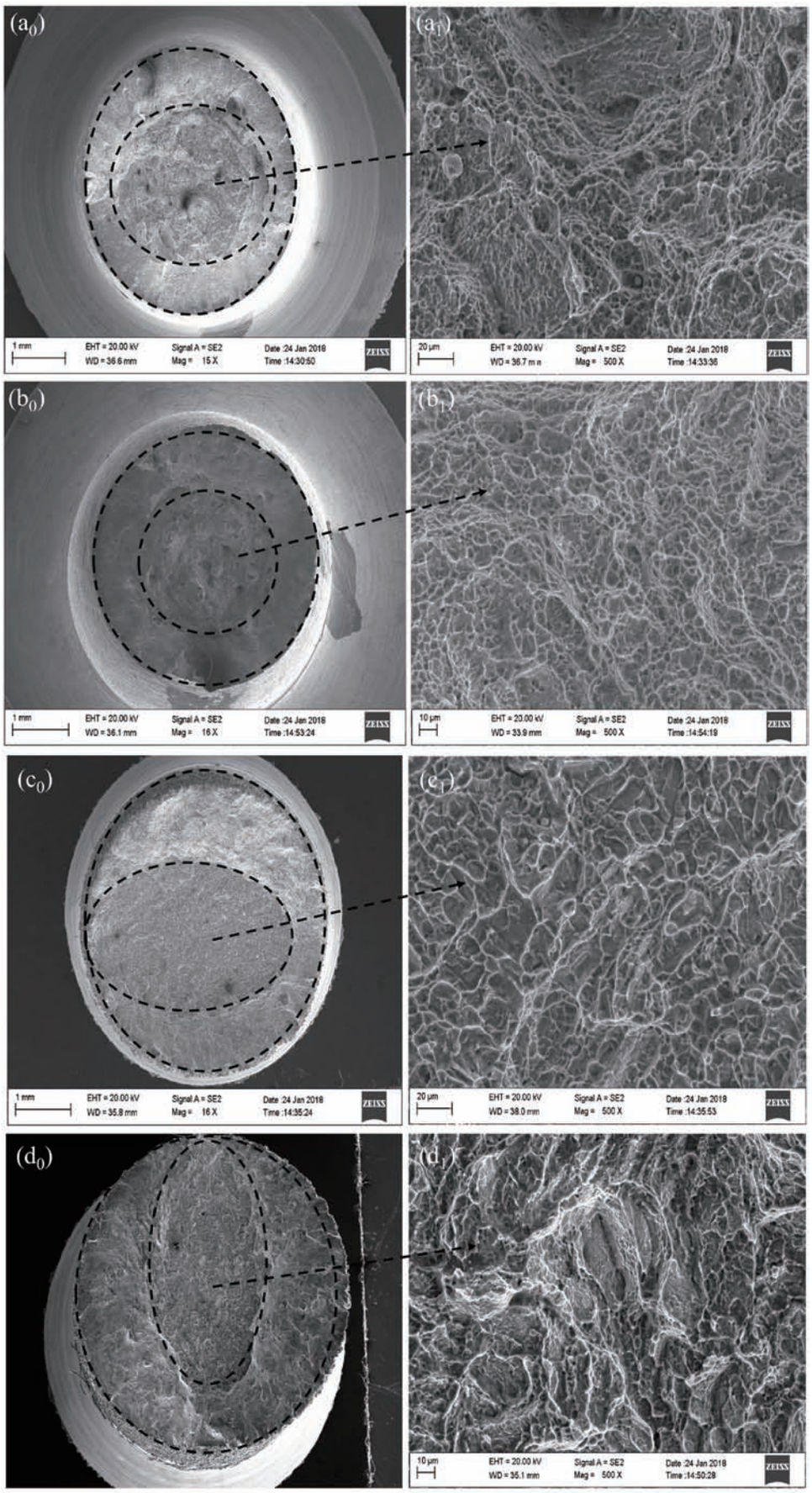

Fig. 8: Some typical low and high magnification images of fracture morphology of vertically-built tensile specimens under different conditions: (a_0-a_1) SLM+HT (650 °C/2 h), (b_0-b_1) SLM+HT (800 °C/4 h), (c_0-c_1) SLM+HIP+as-built surface, (d_0-d_1) SLM+as-built surface

in Fig. 8(c_0–d_0). It is well-known that the crack initiation firstly occurs in the center of the specimen and then propagates to the surface along the radial while a cylindrical smooth alloy bar with good plasticity is tensile tested, which results in a circular fiber zone. The ellipse-like fiber zone indicates that the crack initiation takes place at the surface for tensile specimens with an as-built surface. The high magnification fractographic images in the fiber zone are described in Fig. 8(a_1–d_1). It could be seen that the microscopic features of fracture surface depend on the microstructure. For the as-deposited specimens, the tensile fracture surface [Fig. 8(d_1)] is characterized by shallow dimples and opened-up pores. These pores arise from the cracks cutting through the columnar prior-β grains. For the heat-treated specimens, the facture surfaces are covered with different sizes of dimples which originate from the initiation and coalescence of micro-voids. During the tensile test, the stress is not uniformly distributed at the microstructure scale. Locally concentrated stress tends to occur at the interfaces such as α/β phase interfaces and grain boundaries for dislocation pile-up. When the concentrated stress exceeds the interface binding force, micro-voids will occur. The nucleation and growth of microvoids consume a large amount of strain energy. Hence, high density and deep dimples represent a high elongation to failure. The fracture surface after stress relief annealing [Fig. 8(a_1)] is characterized by sparse and shallow dimples, which is consistent with the microstructures and lower ductility, but the fracture surface after annealing at 800 °C for 4 h

[Fig. 8(b_1)] consists of large amounts of dimples. After annealing at 800 °C for 4 h, the matrix is dominated by fine α+β lamellar structures containing a large number of phase interfaces and reducing the stress concentration level at α/β phase interfaces during tensile testing, resulting in higher ductility. Due to the coarse microstructure, the fracture surface of HIP processed samples [Fig. 8(c_1)] shows relatively sparse dimples. The coarse microstructure reduces the nucleation sites of the micro-voids; meanwhile, large α phase lamellae mean a large dislocation slip length which increases the high concentrated stress at α/β phase interfaces, giving rise to low ductility. In addition, due to the presence of notches in the surface, the cracks can quickly propagate through the cross section of samples in the tensile stress without more plastic deformation.

To further reveal the tensile facture mechanism, the crack propagation was analyzed and some typical etched cross sections are shown in Fig. 9. Obvious necking could be observed in machined samples. Although the elongation to failure in the HIP-processed samples with rough surface is comparable to that of as-deposited and machined samples, no noticeable necking was found as described in Fig. 9(d). The differences in matrix structure should be responsible for this phenomena. The ductility of α+β lamellar microstructure is better than that of complete martensite matrix. Building orientation has a significant effect on the fracture behavior in as-deposited samples. The different orientation between tensile load and columnar prior-β grains induces different amounts of grain boundaries exposed to tensile load. In the horizontally built samples, more effective grain boundaries are perpendicular to tensile stress. In the tensile testing, stress concentration takes place at the grain boundaries, which leads to the crack initiation as shown in the circle in Fig. 9(a). The cracks could grow along the grain boundaries. For crack growth along the horizontal direction, the prior-β grains could act as crack barriers. The cracks cut through the columnar grains and a terrace-like crack path is left after tensile testing as depicted in Fig. 9(b). In the machined and HIP-processed samples, once the cracks nucleated, the cracks could propagate along α/β interfaces or across α colonies. The α phase plates also could deflect the direction of crack growth depending on the orientation between crack tip and α colonies [26]. Hence, the crack propagation path in Fig. 9(c) is zigzag. However, for HIP-processed samples with the rough surfaces, the crack could rapidly propagate from the surface to the central area in the tensile stress. The hindrance of α+β lamellar microstructures to crack propagation is negligible under this condition. The path of the crack growth is relatively flat as shown in Fig. 9(d).

3 Conclusions

This work investigated the microstructure, tensile properties and fracture behaviors of SLM-processed Ti-6Al-4V alloy before and after heat treatments. The following conclusions can be drawn:

(1) Because of steep temperature gradient and high cooling rate, the as-deposited microstructures are characterized of columnar grains and fine martensite. Large amounts of dislocations and twins are found in the matrix. The as-deposited properties present high strength, low ductility and obvious anisotropy.

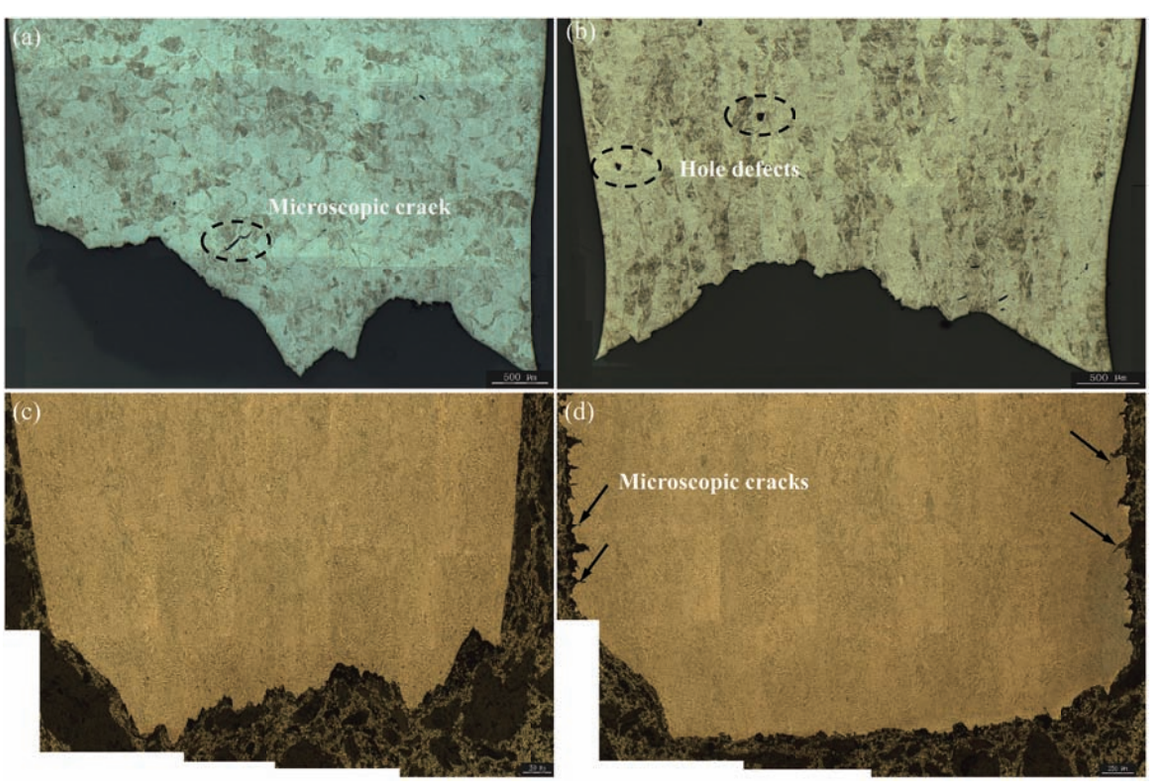

Fig. 9: Optical images of etched cross section through tensile specimens after tensile tests showing the crack growth in as-fabricated and heat treated SLM samples: (a) SLM+H+machined surface, (b) SLM+V +machined surface, (c) SLM+HIP+machined surface, (d) SLM+HIP+as-built surface

(2) After annealing at 800–900°C for 2–4 h and HIP processing at 920 °C/100 MPa for 2 h, the brittle martensite could be transformed into ductile lamellar (α+β) microstructure and the static tensile properties of SLM processed Ti-6Al-4V alloy after machining could be comparable to that of wrought materials and the anisotropy of mechanical properties could be eliminated.

(3) As-built surfaces have great detrimental influences to the mechanical properties of SLM processed Ti-6Al-4V alloy. The ductility could not meet the minimum ductility requirement of forging even after HIP treatment. The average ductility and reduction of area in the HIP-processed samples with an as-built surface are 9.2% and 20%, respectively.

(4) The tensile fracture behaviors of SLM-processed Ti-6Al-4V alloy depend on the building direction, microstructure and surface condition. In as-fabricated samples, the different direction between tensile load and columnar grains gives rise to different tensile fracture behavior. The cracks could nucleate at the columnar grain boundaries and the columnar grains could act as hindrances for crack propagation in the horizontal direction. In heat-treated and machined samples, the α+β lamellar microstructures could hinder or distort the crack propagation path. The crack initiation occurs at the surface in the tensile samples with an as-built surface.

References

[1] Antonysamy A A. Microstructure, texture and mechanical property evolution during additive manufacturing of Ti6Al4V alloy for aerospace applications. Ph.D.Thesis. England: University of Manchester, 2012: 33–39.

[2] Thijs L, Verhaeghe F, Craeghs T, et al. A study of the microstructural evolution during selective laser melting of Ti-6Al-4V. Acta Materialia, 2010, 58(9): 3303–3312.

[3] Simonelli M, Tse Y Y, Tuck C. Effect of the build orientation on the mechanical properties and fracture modes of SLM Ti-6Al-4V. Materials Science and Engineering A, 2014, 616: 1–11.

[4] Qiu C, Adkins N J, Attallah M M. Microstructure and tensile properties of selectively laser-melted and of HIPed laser-melted Ti-6Al-4V. Materials Science and Engineering A, 2013, 578: 230–239.

[5] Yang J, Yu H, Yin J, et al. Formation and control of martensite in Ti-6Al-4V alloy produced by selective laser melting. Materials & Design, 2016, 108: 308–318.

[6] Yang J, Yu H, Wang Z, et al. Effect of crystallographic orientation on mechanical anisotropy of selective laser melted Ti-6Al-4V alloy. Materials Characterization, 2017, 127: 137–145.

[7] Zaeh M F, Branner G. Investigations on residual stresses and deformations in selective laser melting. Production Engineering, 2010, 4(1): 35–45.

[8] Xu W, Brandt M, Sun S, et al. Additive manufacturing of strong and ductile Ti-6Al-4V by selective laser melting via in situ martensite decomposition. Acta Materialia, 2015, 85: 74–84.

[9] Ali H, Ma L, Ghadbeigi H, et al. In-situ residual stress reduction, martensitic decomposition and mechanical properties enhancement through high temperature powder bed pre-heating of Selective Laser Melted Ti6Al4V. Materials Science and Engineering A, 2017, 695: 211–220.

[10] Vilaro T, Colin C, Bartout J-D. As-fabricated and heat-treated microstructures of the Ti-6Al-4V alloy processed by selective laser melting. Metallurgical and Materials Transactions A, 2011, 42(10): 3190–3199.

[11] Sallica-Leva E, Caram R, Jardini A, et al. Ductility improvement due to martensite α′ decomposition in porous Ti-6Al-4V parts produced by selective laser melting for orthopedic implants. Journal of the Mechanical Behavior of Biomedical Materials, 2016, 54: 149–158.

[12] Yadroitsev I, Krakhmalev P, Yadroitsava I. Selective laser melting of Ti6Al4V alloy for biomedical applications: Temperature monitoring and microstructural evolution. Journal of Alloys and Compounds, 2014, 583: 404–409.

[13] Kahlin M, Ansell H, Moverare J. Fatigue behaviour of additive manufactured Ti6Al4V, with as-built surfaces, exposed to variable amplitude loading. International Journal of Fatigue, 2017, 103: 353–362.

[14] Kahlin M, Ansell H, Moverare J. Fatigue behaviour of notched additive manufactured Ti6Al4V with as-built surfaces. International Journal of Fatigue, 2017, 101: 51–60.

[15] GB/T 228-2010. Metallic materials-tensile testing at ambient temperature.

[16] Zhong H, Zhang X, Wang S, et al. Examination of the twinning activity in additively manufactured Ti-6Al-4V. Materials & Design, 2018, 144: 14–24.

[17] Mur F G, Rodriguez D, Planell J. Influence of tempering temperature and time on the α′-Ti-6Al-4V martensite. Journal of Alloys and Compounds, 1996, 234(2): 287–289.

[18] Semiatin S, Kirby B, Salishchev G. Coarsening behavior of an alpha-beta titanium alloy. Metallurgical and Materials Transactions A, 2004, 35(9): 2809–2819.

[19] ASTM F1472-14,Standard Specification for Wrought Titanium-6Aluminum-4Vanadium Alloy for Surgical Implant Applications.

[20] Cao S, Chu R, Zhou X, et al. Role of martensite decomposition in tensile properties of selective laser melted Ti-6Al-4V. Journal of Alloys and Compounds, 2018, 744: 357–363.

[21] Lütjering G. Influence of processing on microstructure and mechanical properties of (α+ β) titanium alloys. Materials Science and Engineering A, 1998, 243(1-2): 32–45.

[22] Wei K, Wang Z, Zeng X. Effect of heat treatment on microstructure and mechanical properties of the selective laser melting processed Ti-5Al-2.5 Sn α titanium alloy. Materials Science and Engineering A, 2018, 709: 301–311.

[23] Mertens A, Reginster S, Paydas H, et al. Mechanical properties of alloy Ti-6Al-4V and of stainless steel 316L processed by selective laser melting: influence of out-of-equilibrium microstructures. Powder Metallurgy, 2014, 57(3): 184–189.

[24] Carroll B E, Palmer T A, Beese A M. Anisotropic tensile behavior of Ti-6Al-4V components fabricated with directed energy deposition additive manufacturing. Acta Materialia, 2015, 87: 309–320.

[25] Sun Y, Gulizia S, Oh C, et al. The influence of As-Built surface conditions on mechanical properties of Ti-6Al-4V additively manufactured by selective electron beam melting. JOM, 2016, 68(3): 791–798.

[26] Galarraga H, Warren R J, Lados D A, et al. Fatigue crack growth mechanisms at the microstructure scale in as-fabricated and heat treated Ti-6Al-4V ELI manufactured by electron beam melting (EBM). Engineering Fracture Mechanics, 2017, 176: 263–280.

This work was financially supported by the National Program on Key Basic Research Project of China (973 Program) under Grant (No. 613281), the National Natural Science Foundation of China (No.51505451), and the Natural Science Foundation of Beijing (No.3172042). This work has also been supported by EMUSIC which is part of an EU-China collaboration and has received funding from the European Union's Horizon 2020 research and innovation programme under Grant Agreement No. 690725 and from MIIT under the programme number MJ-2015-H-G-104.